ACS OMEGA

http://pubs.acs.org/journal/acsodf

Article

Psilocybin: Characterization of the Metastable Zone Width (MSZW), Control of Anhydrous Polymorphs, and Particle Size Distribution (PSD)

Robert B. Kargbo,* Alexander M. Sherwood, Poncho Meisenheimer, Kelsey Lenoch, and Solomon Abebe

Cite This: *ACS Omega* 2022, 7, 5429−5436

Read Online

ACCESS | Metrics & More | Article Recommendations | Supporting Information

ABSTRACT: Psilocybin, a serotonergic agonist, was granted a "breakthrough therapy" status by the Food and Drug Administration for clinical trials involving major depressive disorder and treatment-resistant depression. The direct phosphorylation of psilocin to psilocybin that uses a fast crystallization associated with a kinetically controlled process resulted in a smaller particle size distribution. Herein, the measurement of the metastable zone width (MSZW) and nucleation induction enabled a thermodynamically controlled crystallization process, which leads to the formation of a crystal structure with stronger interactions, controlled particle size distribution (PSD), and improved impurity profile. Employing a high-resolution inline microscopy viewer allowed the real-time monitoring of the crystallization process and the measurement of the particle size. We also present a comprehensive study of the formation of polymorph B (trihydrate), polymorph A (anhydrate), and polymorph H (anhydrate) using water recrystallization, which indicates that the formation of polymorph B (trihydrate) is independent of the crystallization method. However, polymorphs A and H are dependent on the mode of drying: drying at room temperature under vacuum gives rise to mainly polymorph A, and when heated even at relatively low temperatures, a mixture of polymorphs A and H beings to form.

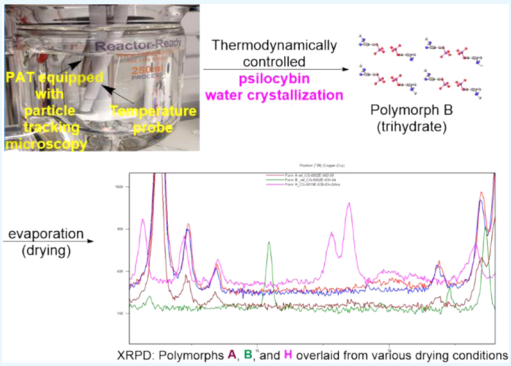

INTRODUCTION

The quest for an ideal crystallization process in the past has been enigmatic but has become a very commonly used separation process in many different industries, including materials and pharmaceutical industries.[1−4] More than 90% of active pharmaceutical ingredients (APIs) are synthesized as crystalline solid products.[5,6] The crystal form has become essential to explore the design of crystal engineering techniques that anticipate probable intermolecular interactions and desired new solid forms with required properties.[7]

In this regard, we aimed to investigate the applicability of a crystal engineering technique that improves the physicochemical properties of psilocybin API. Psilocybin, consumed by humans for thousands of years, according to archeological evidence,[8] has demonstrated potential therapeutic utility in conjunction with an environment of psychological support. In over 70 registered clinical trials, studies have focused on its antidepressant effects on patients with cancer, major depressive disorder, treatment-resistant depression, and other diverse indications.[9−11] The second-generation kilogram-scale synthesis of psilocybin was recently reported, which addresses several challenges first encountered with the scale-up of previously described literature procedures.[12] The final purification employed sequential reslurry of API in methanol, followed by reslurry in warm water to minimize degradation. The isolated crystalline trihydrate was dried to obtain the anhydrous polymorphic API that requires sieving during drug product manufacturing due to agglomerations and the poor flow property of the powder. Therefore, the aim of our study is to achieve the following.

First, the determination of the metastable zone width (MSZW) during the crystallization process.[13,14] Given the known hydrolysis of psilocybin to psilocin, process parameters such as seeding temperature, cooling rate, stirring speed, and other parameters require appropriate engineering controls to achieve consistency and reproducibility of the crystals.

Second, control of polymorphs such that a single desired polymorph is consistently produced at a large scale had been a challenge. Herein, we report the systematic evolution of engineering controls that yield pure anhydrous polymorph A as

Received: November 29, 2021
Accepted: January 17, 2022
Published: February 7, 2022

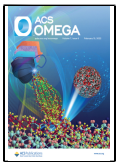

© 2022 The Authors. Published by American Chemical Society

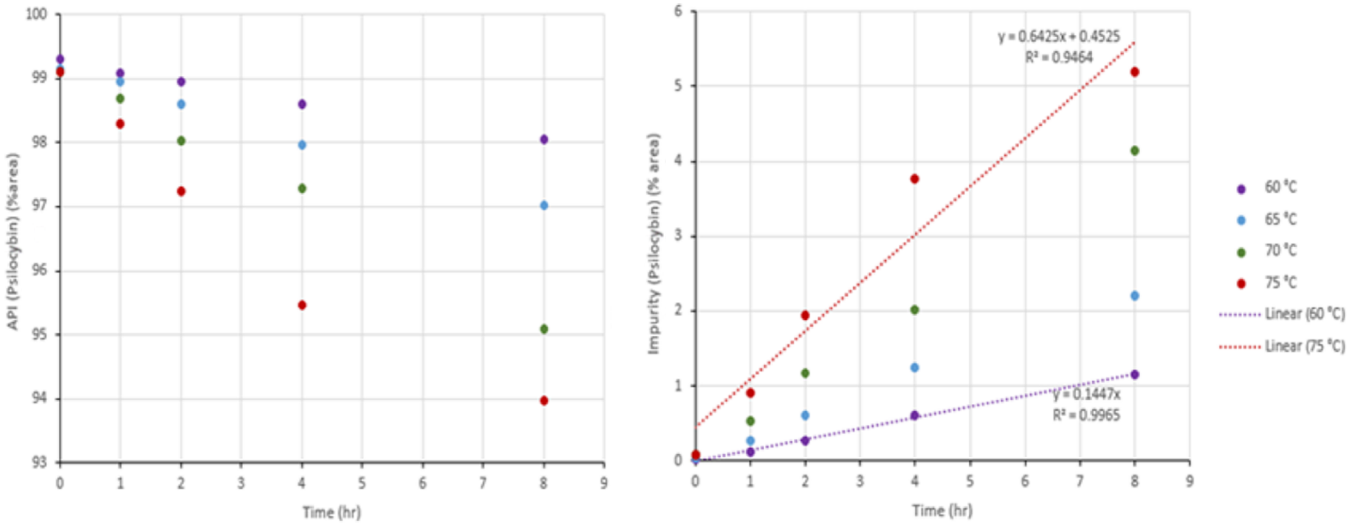

Figure 1. Area % from ultra-performance liquid chromatography (UPLC) for psilocybin and impurity peaks.

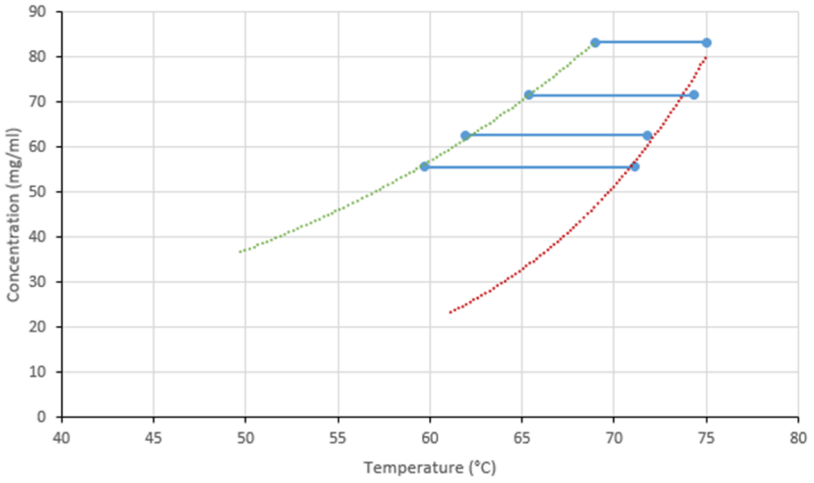

Figure 2. Metastable zone width data for psilocybin. Solid blue line: measured MSZW, dotted green line: estimated T_{cryst} profile, dotted red line: estimated T_{diss} profile.

a single reproducible polymorph at a large scale. The control of polymorphism and particle size is an essential concern to the *in vivo* performance and manufacturability of an API. These important properties can influence key material attributes such as crystal surface energetics,[15] dissolution rate,[16,17] and powder flowability.[18−21]

Third, there was the need to control the PSD, which is well known in the industry.[22−25] However, an efficient method such as dry milling using a fluid energy mill or mechanical impact comes with an increased cost of processing and a potential decrease in yield. Due to the significant mass loss on dehydration of the trihydrate polymorph, the anhydrous polymorph crystal has been observed as fragile. The fragility of the crystals poses a formidable challenge as process handling has to be carefully studied. Irrespective of the sizes of the produced trihydrate crystals, anhydrous crystals will lead to a small PSD during the process and transport of the API. In a previous manufacturing campaign, the fine particle size (d_{50} = ~10.9 μm) of the API led to an increase in the surface area and significant agglomeration that had a negative impact during encapsulation. This also entails a suitable analytical method such as laser light diffraction that gives specific PSD determination. Furthermore, the API must meet the targeted physicochemical properties and specifications that ensure reproducibility.[26]

RESULTS AND DISCUSSION

Hydrolysis Investigation. Previously reported degradation of psilocybin to psilocin during synthesis and crystallization had not been fully quantified. To characterize the MSZW, the hydrolysis process had to be understood and quantified to enable a consistent purity profile of the manufactured API. The rate of degradation at various process temperatures in an aqueous solution was determined, and samples were collected at 0, 1, 2, 4, and 8 h for each experiment, as shown in Figure 1. These experiments suggest the rate of hydrolysis can be approximated as a constant rate, ranging from 0.14%/h at 60 °C to 0.64%/h at 75 °C. In addition, the effect of time and temperature surmises that time is the critical parameter with nearly 3 times higher effect compared to temperature.[27] This indicated that a higher dissolution temperature, up to a maximum of 75 °C, was preferable since it reduced the time above the hydrolysis threshold.

https://doi.org/10.1021/acsomega.1c06708
ACS Omega 2022, 7, 5429−5436

Metastable Zone Width (MSZW) Determination. Having established a predictive relationship between psilocybin degradation, time, and solution temperature, we set out to characterize the MSZW using an infrared (IR) transmission probe. The formation of a nanoscopic small crystal nucleus still remains a mystery; however, indirect methods to measure nucleation kinetics have been developed.[28] According to classical nucleation theory (CNT), small concentration fluctuations in a supersaturated liquid cause the formation of small and extremely unstable embryos crystals, most of which will dissolve again, but those in regions of local high supersaturations can continue to grow and reach the critical size by overcoming the free energy barrier. Generally, a certain time elapses between the generation of supersaturation and detection of the first crystals in the solution, which is the metastable state. There are two kinetic properties that quantify the ability of the system to remain in this metastable state, i.e., the MSZW and the induction time.[29,30] Data from the sample vials, dissolution, and precipitation events were recorded as the point of complete transmission of IR and the onset of turbidity with an IR probe. Experiments were carried out at a fast-cooling rate (1 °C/min) to determine its effects on the MSZW. These experiments showed only a slightly lower crystallization onset temperature (T_{cryst}) and a much higher variability of dissolution temperature (T_{diss}). The estimated T_{diss}, T_{cryst}, and MSZW can be seen in Figure 2, and the data are tabulated in the Supporting Information. As seen in Figure 2, three regions exist: (1) the labile zone (prior to the dotted green line), which contains the supersaturated region with spontaneous homogeneous nucleation and growth; (2) the metastable zone (between the dotted green line and the dotted red line), which is the supersaturated region with growth and no homogeneous spontaneous nucleation; and (3) the stable zone (beyond the dotted red line), which is the undersaturated region with no crystallization.

A slight increase in the process volume leads to a slight decrease in the dissolution temperature but could result in a larger reduction in the seed temperature. To determine the effect of this increase in volume on product yield, equilibrium solubility estimations were carried out at 20 and 5 °C by slurrying for 24 h in water at each temperature. The concentration was determined by UPLC, and solids were also isolated from these solubility slurries and analyzed by XRPD to determine whether there were any changes in form at the lower temperature. There was no change in trihydrate (Form B), and the solubility at each temperature was determined along with solubility estimates, using aliquoted addition at higher temperatures.[31] The use of aliquot addition as opposed to equilibrium solubility for these higher temperatures circumvented the hydrolysis of psilocybin since it would have obscured the measurements for equilibrium solubility. The established MSZW for psilocybin improves the design and control of crystallization processes and offers insights into the mechanism of nucleation.

Control of PSD during Crystallization. A Design of Experiment (DoE), which consists of two factors and three levels, was conducted, taking seed temperature and seed loading as factors and particle size as the response variable. The initial indication of the fragility of the crystalline solid necessitated the need to switch the analytical measurement from laser light diffraction to microscopic analysis. Consequently, using a Keyence VHX-1000E microscope, the particle size was measured by calculating the diameter of an equivalent circle (by area) for approximately 1000 particles per sample and using the average of these measurements. These results are displayed in Table 1 and are presented as a contour

Table 1. Particle Size of Form B as Measured with a Keyence VHX-1000E Microscope

entry	seed temperature (°C)	seed loading (% w/w)	diameter of an equivalent circle (μM)
1	70	0.1	23.2
2	70	0.5	20.1
3	70	1	18.2
4	67	0.1	19.6
5	67	0.5	18.7
6	67	1	17.6
7	64	0.1	14.1
8	64	0.5	15.8
9	64	1	12

plot in Figure 3 generated using JMP 15 statistical software. These data suggest that particle size growth is positively related to temperature but negatively impacted by seed loading. As shown in Table 1, there is a steady decrease in particle size as the seed loading is increased; this is also illustrated in the contour plot shown in Figure 3. In general, the size and number of seed particles added determine the available surface area for crystal growth. If large crystals are desired, then fewer seed particle loadings are utilized.[32] Figure 4 shows the microscopy images of samples taken to correlate various seeding temperatures and seed loadings during the crystallization process. The effect of seed loading was lessened as the seed temperature decreased, possibly due to the fact that the crystallization likely became nucleation-dominated at lower seeding temperatures due to a higher supersaturation ratio. Microscopy images (Figure 4) show the formation of large crystals, which led to over fourfold improvement in PSD (d_{50} = ~47.9 μm) compared to the previous synthesis.

Effect of Powder Bed Density on Drying and Polymorph Interconversion. Controlling the PSD and polymorph required the implementation of multiple techniques, such as the use of *in situ* process analytical technology (PAT), which aids in a mechanistic understanding of the crystallization processes and process design. Notably, this work showcases the importance of studying the impact of drying on particle properties such as brittleness, polymorphism, cohesiveness, and so on. Ostwald's law of the emergence of thermodynamically stable crystal forms states that the least stable crystal form is likely to crystallize first, which is often governed by controlling crystallization conditions such as supersaturation, nucleation kinetics, and temperature.[33] However, not all crystal forms follow such a natural pattern. For example, regular table salt (sodium chloride) harvested from sea water has two stable naturally occurring polymorphic forms. Only recently, four new polymorphs were experimentally found; however, they were unstable.[34] Analogously, psilocybin has two naturally occurring relatively stable Forms (trihydrate B and anhydrous A) when isolated from aqueous media and a Form H isolated at higher temperatures during drying.[35] Psilocybin's propensity to form solvates with several solvents and selection of a crystallization system have been recently evaluated.[36,37] The isolation and characterization of less-stable crystal forms can be quite challenging to manufacture in a consistent and controlled manner.[38] The

https://doi.org/10.1021/acsomega.1c06708
ACS Omega 2022, 7, 5429−5436

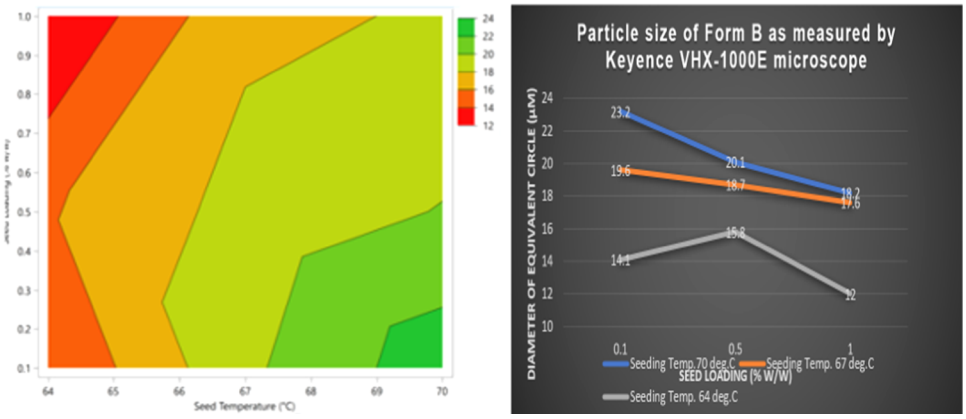

Figure 3. Contour plot of the particle size at various seed loadings, equivalent circles, and temperatures.

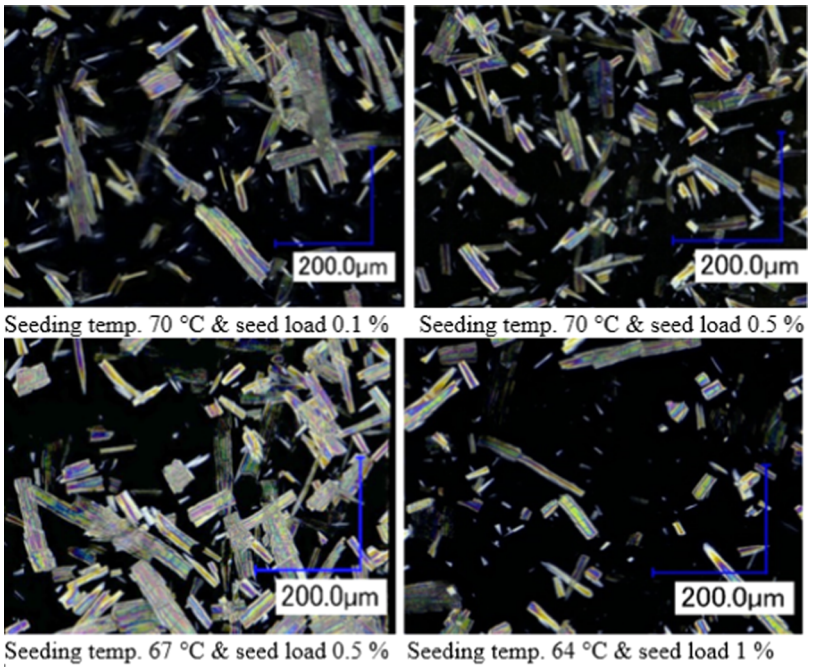

Figure 4. Microscopy images of samples taken at various seeding temperatures and seed loadings.

use of in-process analytical tools to gain a better understanding of the crystallization process proved to be an invaluable strategy.

It was thought that the bulk density and/or solid depth of the material during the drying process could facilitate conditions conducive to pattern H formation. To test this hypothesis, two crystallization experiments at a 3.0 g scale were carried out to afford the trihydrate polymorph (Form B).[31] Prior to drying, the isolated solid was densely packed into a PP/nylon (polypropylene, polyester, and nylon) liner with a cake bed thickness of approximately 25 mm, while the material from the second experiment was spread out in a borosilicate glass dish to a bed thickness of approximately 5 mm and placed into a PP/nylon liner. Both containers were dried under vacuum at elevated temperatures.

During the drying process, form analysis was carried out by X-ray powder diffraction (XRPD) on samples taken from the densely packed sample at two points, i.e., at the core and edge of the powder mass. XRPD patterns showed complete conversion from Form B to Form A after only 6 h, but they also showed trace amounts of pattern H. The samples were taken from the outer edge of the powder mass, as well as from the central core of the powder mass. Both samples showed the same pattern, indicating that the conditions for pattern H formation are not localized within the powder mass and, at least at this scale, are consistent throughout. On the other hand, on the thinly spread sample, XRPD results showed complete conversion from Form B to Form A, after 6 h; however, with this experiment, there was no trace of pattern H. The sample obtained after 25 h also showed Form A with no trace of pattern H, suggesting that the cake bed thickness is a critical parameter. Furthermore, a separate sample was dried at an ambient temperature under vacuum with no N_2 flow, which again showed only Form A after 36 h. Thermogravimetric analysis exhibited a weight loss of 0.55% w/w, well within the desired specification for water content. The process of obtaining consistent and the single desired polymorph A required significant drying time and the thin spread of the API during the drying process, which is burdensome to process operations and handling.

To reduce the drying time and temperature, an acetone cake wash was added to the isolation protocol to displace as much

https://doi.org/10.1021/acsomega.1c06708
ACS Omega 2022, 7, 5429−5436

residual water as possible, which should dry faster at the lower temperatures needed. Previous work during the polymorph screening indicated that there were no acetone solvates, and a slurry of Form A in acetone showed no change after 3 days. To test the hypothesis, a 2.0 g sample of Form A was slurried for 3 h in water and was confirmed to have converted to Form B. This slurry was then isolated on a sinter and washed with approximately 3 V water. At this stage, the cake had formed a wet paste, which retained water readily. Half of the filter cake was removed, and this was further split into two portions, one to dry with an N_2 bleed in the oven and one without. A small aliquot sample was also removed at this point and slurried in acetone overnight to check for any form changes; however, this remained as Form B. The remaining filter cake was leveled and washed with 2 x 3 V acetone (Table 2). After the first acetone wash, the cake was a powder with no sign of the previous paste behavior, and after the second acetone wash, the cake was more freely flowing, which suggested a drier powder. The powders were placed into liners, then dried at 35−40 °C at ambient pressure overnight to increase humidity, and N_2 was applied. The experiment was also repeated with vacuum and N_2 being applied immediately. The results can be seen in Table 2, and individual XRPD patterns are shown in Figures 5 and 6. All results showed Form A, suggesting that at this scale, neither acetone wash, N_2 bleed, nor the timing of vacuum application has any effect on pattern H formation. The acetone wash was kept in the isolation protocol due to the reduction in residual moisture and subsequent reduction in the drying time.

Table 2. Drying Conditions and Results for Acetone Wash Experiment

entry	acetone wash	N2 bleed	XRPD form	comment
1	no	no	A	overnight hold at drying temperature but ambient pressure
2	no	yes	A	overnight hold at drying temperature but ambient pressure
3	yes	no	A	overnight hold at drying temperature but ambient pressure
4	no	yes	A	overnight hold at drying temperature but ambient pressure
5	N/A	N/A	B	wet cake sample obtained after acetone wash
6	no	no	A	vacuum applied immediately
7	no	yes	A	vacuum and N_2 applied immediately
8	yes	no	A	vacuum applied immediately
9	yes	yes	A	vacuum and N_2 applied immediately

In addition, the crystallization process was amenable to scale up manufacturing. When 121.8 g of input material was subjected to water crystallization based on the above protocol, an output of 105.3 g (86.5% recovery) and a d_{50} of 40.4 μm were observed.[31]

Particle size distribution (PSD) has a major effect on the probability of meeting content uniformity specifications as a function of formulation dose and a median particle diameter (d_{50}) and is especially critical for low-dose formulations.[39] For API-encapsulation, a narrower PSD would presumably pass content uniformity requirements compared to a broad PSD with a mixture of fine and large particles. Polymorphic crystal forms have become increasingly important in many industries as the need exists to search, identify, and attempt to patent polymorphic forms with favorable properties.[40−45]

Polymorphs that may form during crystallization when the internal molecular and structural arrangement will lead to the diversity of drug crystallinity. This has become increasingly important in the pharmaceutical industry, where polymorphs are reported to change the bioavailability, solubility, and solid stability of the drugs.[46−48] For instance, pemafibrate (an anhydrous drug like psilocybin) selectively activates PPAR α, and it is well known that the crystal form of this drug has a great influence on its bioavailability and efficacy.[49,50]

In the pharmaceutical industry, the polymorphic form of a drug shall be easily produced, compatible with the excipients used in the drug product manufacturing process, and remain

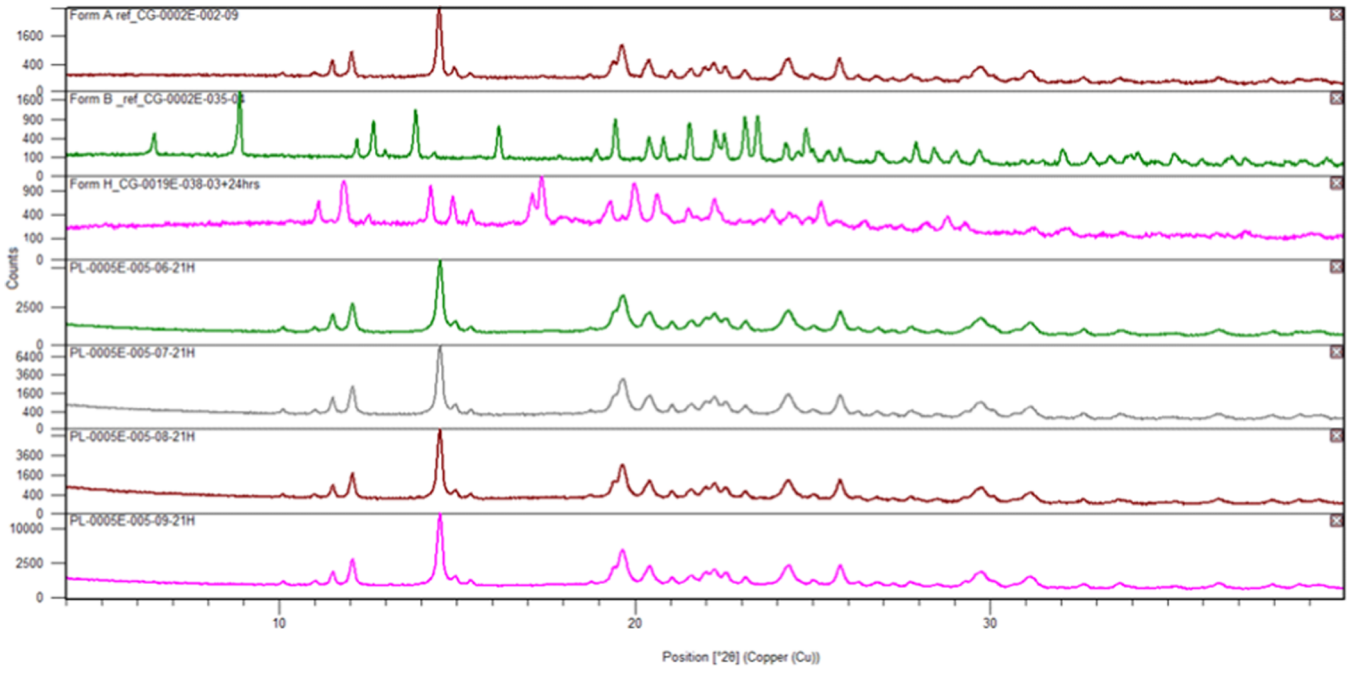

Figure 5. Acetone wash polymorph B dried for 21H and monitored by XRPD.

https://doi.org/10.1021/acsomega.1c06708
ACS Omega 2022, 7, 5429−5436

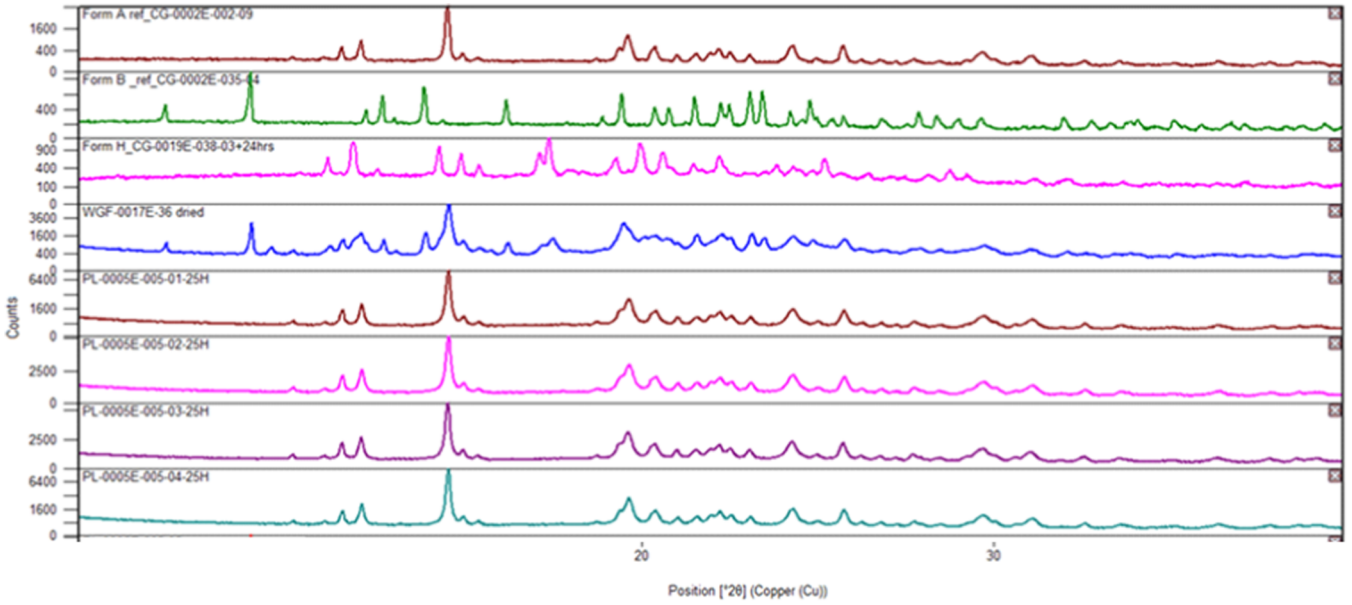

Figure 6. Acetone wash polymorph B dried for 25H and monitored by XRPD.

unchanged for the duration of the drug's shelf life.[51−53] Consequently, many designs of experiments and screening methods are applied to generate potentially the best-suited approaches and stable polymorphs. In bulk crystallization experiments, various strategies are employed, including different solvents,[54,55] seeding,[56] degrees of saturation, varying temperature,[57] process parameter variation, and so on. We report for the first time in psilocybin synthesis a metastable crystallization zone and a drying process that produces a single stable anhydrous polymorphic form.

Major restrictions were placed on developing an API that is suitable for Phase III clinical trials. Consequently, critical material attributes of the API were identified and controlled prior to commercial manufacture. The Phase II API manufactured was produced using slurry and precipitation, and as a consequence, the API demonstrated diminished flowability, which hampered the encapsulation process.

SUMMARY

The goal of determining the MSZW of psilocybin was to optimize the original crystallization process to allow for polishing filtration by decreasing the process concentration that lowers the precipitation temperature and provides a wide enough MSZW, which circumvents precipitation during transfer and filtration. Furthermore, the reduction in concentration also allowed a reduction in seed temperature, reduction of hydrolysis, and subsequent yield loss.

A DoE approach found that the seeding temperature and seed loading were significant factors; however, seed loading had a reduced effect on lower seeding temperatures. In addition, seed loading displayed an inverse relationship with the PSD, whereas seeding temperature showed a positive increase in the PSD. The particle sizes were found to be significantly impacted by the cooling rate, wherein a slow cooling rate yielded a large trihydrate particle size. Furthermore, when the slow cooling rate was combined with a low stirring speed, a large particle size was isolated. However, microscopy analysis pre- and post-isolation confirmed severe particle breakage of the long needle-shaped crystals, which occurred consistently during the filtration and resulted in a change of particle habit to shorter particles and a smaller aspect ratio. Nonetheless, relatively larger particle sizes (d_{50} = ∼47.9 μm) were obtained in this process compared to the previous synthesis that gave particle sizes of ∼10.9 μm. Furthermore, when 121.8 g was subjected to the crystallization process, an output of 105.3 g and a d_{50} of 40.4 μm were observed.

Polymorphs A (anhydrous) and B (trihydrate) were found to be relatively stable and easily formed at lower temperatures compared to polymorph H. Formation of pattern H occurred during drying and was found to be correlated with both oven temperature and drying time.

Laser light diffraction (LLD) was found to be unsuitable for particle size distribution (PSD) determination due to the fragility of the particles and subsequent breakage under even the lowest energy mixing during analysis. The best method for particle size determination for this material was determined to be light microscopy.

EXPERIMENTAL SECTION

Crystallization Process Development. The crystallization experiment was carried out at a gram scale in a HEL Polyblock reactor system, according to the procedure in Table 3. Psilocybin was synthesized based on the previous literature.[12]

X-ray Powder Diffraction (XRPD). XRPD analyses were performed using a Panalytical Empyrean diffractometer equipped with a Cu X-ray tube and a PIXcel 1D-Medipix3 detector system. The samples were analyzed at an ambient temperature in transmission mode and held between low-density PVC films. The Almac default XRPD program was used (range 4−40°2θ, step size of 0.01313°, counting time of 92 s, ∼20 min run time). The samples were spun at 60 rpm during data collection. XRPD patterns were sorted and manipulated using HighScore Plus v4.9 software.

Particle Size Distribution (PSD). Particle size analysis (PSA) was carried out using a wet dispersion method with parameters outlined in Table 4 on a Malvern Master Sizer 3000.

https://doi.org/10.1021/acsomega.1c06708
ACS Omega 2022, 7, 5429−5436

Table 3. Procedure for Crystallization Experiment

step	description
1	charge psilocybin (5 g) to water (14 V) at 75 °C
2	hold 10 min or until dissolution
3	cool down to 69 °C
4	add seed material in 0.1 V water
5	cool down to 40 °C at 10 °C/h
6	cool down to 5 °C at 5 °C/h
7	hold for 9.5 h
8	filter reactor contents
9	charge water (1 V) wash
10	charge water (2 V) wash
11	portion wet cake for drying experiments
12	dry at respective drying conditions for up to 90 h

Table 4. PSA Instrument Parameters

parameter	value
sample unit	hydro MV
particle type	nonspherical particle mode
scattering model	Mie
particle refractive index (red and blue light)	1.644
particle absorption index (red and blue light)	0.01
dispersant name	heptane
dispersant refractive index	1.390
background measurements (red and blue light)	10 s
sample measurements (red and blue light)	10 s
number of measurements	three measurement cycles per sample
delay between measurements	0 s
% obscuration	low limit: 10%, high limit: 15%.
stirrer speed	2250 rpm
analysis model and sensitivity	general purpose and normal

■ ASSOCIATED CONTENT

Supporting Information

The Supporting Information is available free of charge at https://pubs.acs.org/doi/10.1021/acsomega.1c06708.

An outline of the hydrolysis of psilocybin at various temperatures in an aqueous solution; metastable zone width experimental data; drying experiment on the interconversion of polymorph Form B to Form A at various temperatures; and recrystallization at various seed loadings (PDF)

■ AUTHOR INFORMATION

Corresponding Author

Robert B. Kargbo − *Usona Institute, Madison, Wisconsin 53711, United States;* orcid.org/0000-0002-5539-6343; Email: kargborb@gmail.com

Authors

Alexander M. Sherwood − *Usona Institute, Madison, Wisconsin 53711, United States;* orcid.org/0000-0003-0895-0791

Poncho Meisenheimer − *Usona Institute, Madison, Wisconsin 53711, United States*

Kelsey Lenoch − *Usona Institute, Madison, Wisconsin 53711, United States*

Solomon Abebe − *Almac Sciences, Craigavon BT63 5QD, United Kingdom*

Complete contact information is available at: https://pubs.acs.org/10.1021/acsomega.1c06708

Notes

The authors declare no competing financial interest.

■ ACKNOWLEDGMENTS

The authors thank William Linton for his foresight, intuition, and support.

■ REFERENCES

(1) Orehek, J.; Teslic, D.; Likozar, B. Continuous Crystallization Processes in Pharmaceutical Manufacturing: A Review. *Org. Process Res. Dev.* **2021**, *25*, 16−42.

(2) Nyvlt, J.; Söhnel, O.; Matachová, M.; Broul, M. *The Kinetics of Industrial Crystallization*; Elsevier Science Publishers, 1985.

(3) Tavare, N. S. *Crystallization Kinetics. Industrial Crystallization*; Springer International Publishing, 1995; Chapter 3, pp 57−78.

(4) Garside, J.; Mersmann, A.; Nyvlt, J. *Measurement of Crystal Growth and Nucleation Rates*, 2nd ed.; Institution of Chemical Engineers, 2002.

(5) Chen, J.; Sarma, B.; Evans, J. M. B.; Myerson, A. S. Pharmaceutical Crystallization. *Cryst. Growth Des.* **2011**, *11*, 887.

(6) Yu, Z. Q.; Chew, J. W.; Chow, P. S.; Tan, R. B. H. Recent Advances in Crystallization Control. *Chem. Eng. Res. Des.* **2007**, *85*, 893.

(7) Kundu, S.; Kumari, N.; Soni, S. R.; Ranjan, S.; Kumar, R.; Sharon, A.; Ghosh, A. Enhanced Solubility of Telmisartan Phthalic Acid Cocrystals within the pH Range of a Systemic Absorption Site. *ACS Omega* **2018**, *3*, 15380.

(8) Samorini, G. The Oldest Representations of Hallucinogenic Mushrooms in the World. *Integration* **1992**, *2*, 69−78.

(9) Romeo, B.; Hermand, M.; Petillion, A.; Karila, L.; Benyamina, A. Clinical and Biological Predictors of Psychedelic Response in the Treatment of Psychedelic and Addictive Disorders: A Systematic Review. *J. Psychiatr. Res.* **2021**, *137*, 273.

(10) De Gregorio, D.; Aguilar-Valles, A.; Preller, K. H.; Heifets, B. D.; Hibicke, M.; Mitchell, J.; Gobbi, G. Hallucinogens in Mental Health: Preclinical and Clinical Studies on LSD, Psilocybin, MDMA, and Ketamine. *J. Neurosci.* **2021**, *41*, 891.

(11) https://clinicaltrials.gov/ct2/results?cond=psilocybin&term=&cntry=&state=&city=&dist= (accessed May 31, 2021).

(12) Kargbo, R. B.; Sherwood, A.; Walker, A.; Cozzi, N. V.; Dagger, R. E.; Sable, J.; O'Hern, K.; Kaylo, K.; Patterson, T.; Tarpley, G.; Meisenheimer, P. *ACS Omega* **2020**, *5*, 16959.

(13) Chen, J.; Sarma, B.; Evans, J. M. B.; Myerson, A. S. Pharmaceutical Crystallization. *Cryst. Growth Des.* **2011**, *11*, 887.

(14) Alvarez, A. J.; Myerson, A. S. Continuous Plug Flow Crystallization of Pharmaceutical Compounds. *Cryst. Growth Des.* **2010**, *10*, 2219.

(15) Ho, R.; Wilson, D. A.; Heng, P. Y. Y. Crystal habits and the variation in surface energy heterogeneity. *Cryst. Growth Des.* **2009**, *9*, 4907.

(16) Chu, K. R.; Lee, E.; Jeong, S. H.; Park, E. S. Effect of particle size on the dissolution behaviors of poorly water-soluble drugs. *Arch. Pharm. Res.* **2012**, *35*, 1187.

(17) Mosharraf, M.; Nyström, C. The effect of particle size and shape on the surface specific dissolution rate of microsized practically insoluble drugs. *Int. J. Pharm.* **1995**, *122*, 35.

(18) Sandler, N.; Wilson, D. Prediction of granule packing and flow behavior based on particle size and shape analysis. *J. Pharm. Sci.* **2010**, *99*, 958.

(19) Kaerger, J. S.; Edge, S.; Price, R. Influence of particle size and shape on flowability and compactibility of binary mixtures of

paracetamol and microcrystal line cellulose. *Eur. J. Pharm. Sci.* **2004**, *22*, 173.
(20) Wilson, D.; Bunker, M.; Milne, D.; Jawor-Baczynska, A.; Powell, A.; Blyth, I.; Streather, D. Particle engineering of needle shaped crystals by wet milling and temperature cycling: optimization for roller compaction. *Powder Technol.* **2018**, *339*, 641.
(21) Liu, L. X.; Marziano, I.; Bentham, A. C.; Litster, J. D.; White, E. T.; Howes, T. Effect of particle properties on the flowability of ibuprofen powders. *Int. J. Pharm.* **2008**, *362*, 109.
(22) Nakach, M.; Authelin, J. -R.; Corsini, C.; Gianola, G. Jet milling industrialization of sticky active pharmaceutical ingredient using quality by-design approach. *Pharm. Dev. Technol.* **2019**, *24*, 849.
(23) Midoux, N.; Hosek, P.; Pailleres, L.; Authelin, J. R. Micronization of pharmaceutical substances in a spiral jet mill. *Powder Technol.* **1999**, *1*, 113.
(24) Nakach, M.; Authelin, J-R.; Chamayou, A.; Dodds, J. Comparison of various milling technologies for grinding pharmaceutical powders. *Int. J. Miner. Process.* **2004**, *74*, S173.
(25) Bonakdar, T.; Ghadiri, M. Analysis of pin milling of pharmaceutical materials. *Int. J. Pharm.* **2018**, *552*, 394.
(26) Sun, Z.; Ya, N.; Adams, R. C.; Fang, F. S. Particle size specifications for solid oral dosage forms: a regulatory perspective. *Am. Pharm. Rev.* **2010**, *13*, 68.
(27) See Supporting information.
(28) Jiang, S.; Ter Horst, J. H. Crystal Nucleation Rates from Probability Distributions of Induction Times. *Cryst. Growth Des.* **2011**, *11*, 256−261.
(29) Kashchiev, D.; Verdoes, D.; van Rosmalen, G. M. Induction Time and Metastability Limit in New Phase Formation. *J. Cryst. Growth* **1991**, *110*, 373−380.
(30) Devos, C.; Gerven, T.; Kuhn, S. A Review of Experimental Methods for Nucleation Rate Determination in Large-Volume Batch and Microfluidic Crystallization. *Cryst. Growth Des.* **2021**, *21*, 2541.
(31) Supporting information.
(32) Laird, T. Book Review of Crystallization − Basic Concepts and Industrial Applications. *Org. Process Res. Dev.* **2013**, *17*, 884.
(33) Dunitz, J. D.; Bernstein, J. Disappearing Polymorphs. *Acc. Chem. Res.* **1995**, *28*, 193−200.
(34) Kaupp, G. Six Polymorphs of Sodium Chloride upon Depth-Sensing Macroindentation with Unusual Long-Range Cracks Requiring 30 N Load. *J. Mater. Sci. Eng.* **2018**, *7*, 4.
(35) Londesbrough, D. J.; Brown, C.; Northen, J. S.; Moore, G.; Patil, H.; Nichols, D. Preparation of Psilocybin, Different Polymorphic Forms, Intermediates, Formulations and Their Use. WO Patent WO2019/073379A1 2019.
(36) Greenan, C.; Arlin, J.; Lorimer, K.; Kaylo, K.; Kargbo, R.; Meisenheimer, P.; Tarpley, G. W.; Sherwood, A. Preparation and Characterization of Novel Crystalline solvates and Polymorphs of Psilocybin and Identification of Solid Forms Suitable for Clinical Development. Preprint DOI: 10.13140/RG.2.2.32357.14560.
(37) Sherwood, A. M.; Kargbo, R. B.; Kaylo, K. W.; Cozzi, N. V.; Meisenheimer, P.; Kaduk, J. A. Psilocybin: crystal structure solutions enable phase analysis of prior art and recently patented examples. *Acta Crysta.* **2022**, *78*, 36.
(38) Chemburkar, S. R.; Bauer, J.; Deming, K.; Spiwek, H.; Patel, K.; Morris, J.; Henry, R.; Spanton, S.; Dziki, W.; Porter, W.; Quick, J.; Bauer, P.; Donaubauer, J.; Narayanan, B. A.; Soldani, M.; Riley, D.; McFarland, K. Dealing with the impact of Ritonovir Polymorphs on the Late Stages of Bulk Drug Process Development. *Org. Process Res. Dev.* **2000**, *4*, 413−417.
(39) Rohrs, B. R.; Amidon, G. E.; Meury, R. H.; Secreast, P. J.; King, H. M.; Skoug, C. J. Particle size limits to meet USP content uniformity criteria for tablets and capsules. *J. Pharm. Sci.* **2006**, *95*, 1049.
(40) Neumann, M. A.; de Streek, J. V.; Fabbiani, F. P. A.; Hidber, P.; Grassmann, O. Combined crystal structure prediction and high-pressure crystallization in rational pharmaceutical polymorph screening. *Nat. Commun.* **2015**, *6*, No. 7793.
(41) Láng, P.; Kiss, V.; Ambrus, R.; Farkas, G.; Szabo-Revesz, P.; Aigner, Z.; Varkonyi, E. Polymorph screening of an active material. *J. Pharm. Biomed. Anal.* **2013**, *84*, 177.
(42) Allesø, M.; Van Den Berg, F.; Cornett, C.; Jorgensen, F. S.; Halling-Sorensen, B.; De Diego, H. L.; Hovgaard, L.; Aaltonen, J.; Rantanen, J. Solvent diversity in polymorph screening. *J. Pharm. Sci.* **2008**, *97*, 2145.
(43) Jones, A. O. F.; Chattopadhyay, B.; Geerts, Y. H.; Resel, R. Substrate-Induced and Thin-Film Phases: Polymorphism of Organic Materials on Surfaces. *Adv. Funct. Mater.* **2016**, *26*, 2233.
(44) Mensah, J.; Kim, K. J. Polymorph Screening Technology by Controlling Crystallization. *Chem. Eng. Trans.* **2013**, *32*, 2221.
(45) Allesø, M.; Rantanen, J.; Aaltonen, J.; Cornett, C.; van den Berg, F. Solvent subset selection for polymorph screening. *J. Chemom.* **2008**, *22*, 621.
(46) Yamano, M. Approach to Crystal Polymorph in Process Research of New Drug. *J. Synth. Org. Chem., Jpn.* **2007**, *65*, 90.
(47) Foster, J. A.; Damodaran, K. K.; Maurin, A.; Day, G. M.; Thompson, H. P. G.; Cameron, G. J.; Bernal, J. C.; Steed, J. W. Pharmaceutical polymorph control in a drug-mimetic supramolecular gel. *Chem. Sci.* **2017**, *8*, 78.
(48) Miller, J. M.; Collman, B. M.; Greene, L. R.; Grant, D. J. W.; Blackburn, A. C. Identifying the Stable Polymorph Early in the Drug Discovery−Development Process. *Pharm. Dev. Technol.* **2005**, *10*, 291.
(49) Li, L.; Yin, X.; Diao, K. Improving the solubility and Bioavailability of Pemafibrate via a New Polymorph Form II. *ACS Omega* **2020**, *5*, 26245.
(50) Shin, S. Pharmaceutical Composition. WO Patent WO2019004452A12019.
(51) Ehmann, H. M.; Werzer, O. Surface Mediated Structures: Stabilization of Metastable Polymorphs on the Example of Paracetamol. *Cryst. Growth Des.* **2014**, *14*, 3680.
(52) Baraldi, C.; Tinti, A.; Ottani, S.; Gamberini, M. C. Characterization of polymorphic ampicillin forms. *J. Pharm. Biomed. Anal.* **2014**, *100*, 329.
(53) Wang, I. C.; Lee, M. J.; Seo, D. Y.; Lee, H. E.; Choi, Y.; Kim, W. S.; Kim, C. S.; Jeong, M. Y.; Choi, G. J. Polymorph transformation in paracetamol monitored by in-line NIR spectroscopy during a cooling crystallization process. *AAPS PharmSciTech.* **2011**, *12*, 764.
(54) Dichiarante, E.; Curzi, M.; Giaffreda, S. L.; Grepioni, F.; Maini, L.; Braga, D. Crystal forms of the hydrogen oxalate salt of O-desmethylvenlafaxine. *J. Pharm. Pharmacol.* **2015**, *67*, 823.
(55) Allesø, M.; Van Den Berg, F.; Cornett, C.; Jorgensen, F. S.; Halling-Sorensen, B.; De Diego, H. L.; Hovgaard, L.; Aaltonen, J.; Rantanen, J. Solvent diversity in polymorph screening. *J. Pharm. Sci.* **2008**, *97*, 2145.
(56) Braga, D.; Grepioni, F.; Maini, L.; Polito, M.; Rubini, K.; Chierotti, M. R.; Gobetto, R. Hetero-seeding and solid mixture to obtain new crystalline forms. *Chem. - Eur. J.* **2009**, *15*, 1508.
(57) Röthel, C.; Ehmann, H. M. A.; Baumgartner, R.; Reischl, D.; Werzer, O. Alteration of texture and polymorph of phenytoin within thin films and its impact on dissolution. *CrystEngComm* **2016**, *18*, 588.

https://doi.org/10.1021/acsomega.1c06708
ACS Omega 2022, 7, 5429−5436